

The utility of height for the Ediacaran organisms of Mistaken Point

Authors: Emily. G. Mitchell*¹, Charlotte. G. Kenchington^{1,2}.

Affiliations:

¹ Department of Earth Sciences, University of Cambridge, Downing Street, Cambridge, CB2 3EQ, UK.

²Department of Earth Sciences, Memorial University of Newfoundland, 230 Elizabeth Ave, St. John's, NL A1B 3X9, Canada.

*Correspondence to: ek338@cam.ac.uk. Phone: +44 1223 333 416

Ediacaran fossil communities consist of the oldest macroscopic eukaryotic organisms. Increased size (height) is hypothesized to be driven by competition for water-column resources, leading to vertical/epifaunal tiering and morphological innovations such as stems. Using spatial analyses, we find no correlation between tiering and resource competition, and that stemmed organisms are not tiered. Instead, we find height is correlated to greater offspring dispersal, demonstrating the importance of colonization potential over resource competition.

Bedding-plane assemblages of Ediacaran fossils at Mistaken Point, Newfoundland (~566 Ma)¹, are among the oldest known eukaryotic macrofossil communities². In extant marine ecosystems, body size is key to structuring communities, due to size-structured predation dynamics^{3,4}. However, the Mistaken Point communities pre-date macro-predation and (extensive) mobility⁵, and so body size must have played a different role. Instead, the driver of large size has been suggested to be competition for vertically distributed water-column resources, resulting in different taxa occupying different parts of the water column – a process known as tiering⁶. Consequently, tiering to avoid resource competition has been interpreted as the major driver in the diversification of Ediacaran body plans, most notably in the evolution of a non-branched (i.e. “naked”) stem⁷⁻⁹. Since Mistaken Point bedding planes consist of sessile organisms preserved *in-situ*, it is reasonable to assume that approximately all of the macroscopic organisms were preserved, so the bedding planes represent a near-census of the community at the time of burial². Therefore, detailed statistical analyses of these populations and their spatial distributions can be used to determine the relationship between height and resource competition^{10,11}.

We analysed the communities of three large bedding-plane assemblages in the Mistaken Point Ecological Reserve: the ‘D’, ‘E’, and Lower Mistaken Point (LMP) surfaces¹², using the data from [11] (Supplementary Figure 1). These communities are dominated by rangeomorphs, a clade of “fractally-branching” organisms^{13,14,15} with some taxa also possessing a naked stem⁷. These communities also include non-fractally branching frondose arboreomorphs¹⁶; the putative sponge *Thectardis*; fronds awaiting formal description (e.g. “Ostrich Feathers”)²; and irregular bedding-plane features referred to as ivesheadiomorphs and “Lobate Discs”^{2,10,17} (see Methods for details). Community composition differs between the three communities, with the ‘D’ surface notably different due to exclusive population by rangeomorphs with no abundant stemmed taxa (Supplementary Table 2). All three assemblages occur within deep-marine turbidite sequences², with fossils preserved as external moulds in siltstone hemipelagites, cast from above by volcanoclastic deposits¹⁸ (Supplementary Figure 1). A volcanic tuff directly above the ‘E’ surface has been dated to 566.25 ± 0.35 Ma, which provides an upper age constraint on the underlying ‘D’ and LMP surfaces¹⁹.

To quantify the extent of tiering, we calculated the percentage by which each taxon’s population exhibits distinct vertical stratification (*DVS*) with respect to the rest of the community (Supplementary Figure 2). The extent of community tiering is defined as the mean taxa *DVS*. Two different *DVS* metrics were calculated: height-based DVS^{height} and uptake-zone DVS^{uptake} . The taxon-specific DVS^{height} is defined as the percentage of specimens within the taxon population that are not matched in height by any specimen from a different taxonomic group (Supplementary Figure 2). Taxon-specific DVS^{uptake} is defined as the percentage of specimens within a taxon population whose “uptake-zone” (i.e. the branching organism part) is not in the same part of the water column as the uptake-zone of specimens from a different taxonomic group

(Supplementary Figure 2 and Methods). Consequently, $DVS=0\%$ corresponds to no tiering while $DVS=100\%$ corresponds to a completed tiered community.

Competition was detected and quantified using spatial point process analyses, whereby pair correlation functions (PCFs) were calculated to describe the spatial distributions between pairs of taxa on each bedding plane²⁰, with a $PCF=1$ indicating a distribution that was completely spatially random (CSR), $PCF>1$ indicating aggregation, and $PCF<1$ indicating segregation²⁰⁻²². Monte Carlo simulations and Diggle's goodness-of-fit test²² (p_d) were used to indicate significantly non-CSR distributions when the observed PCF deviated outside the simulation envelope coupled with a $p_d<<1$. Where bivariate spatial segregation was detected, partial PCF between size-classes (defined in Methods; Supplementary Figure 3) were calculated, and Diggle's segregation test²³ used to assess segregation of each size class. Identifying the processes behind spatial patterns is not straightforward²²⁻²⁷; however, inter-specific resource competition typically generates a segregated pattern, with segregated largest specimens and CSR or aggregated small specimens²¹. To further investigate the relationship of height with dispersal dynamics, the mean cluster radius was calculated by fitting univariate Thomas cluster models to the univariate PCFs²⁷ (Supplementary Table 4). Linear regressions of these radii were then fitted to mean height, maximum height and mean uptake-zone height for each frondose taxon (Supplementary Table 5).

Only the 'D' surface was found to exhibit high DVS (80.1% , Figure 1, Supplementary Table 1. $DVS^{height}_D=DVS^{uptake}_D$). In contrast, the DVS^{height} for the 'E' surface community is only 12.4%, and only 20.0% for the LMP community (Supplementary Table 1), DVS^{uptake} was larger than DVS^{height} ($DVS^{uptake}_E=44.9\%$; $DVS^{uptake}_{LMP}=40.9\%$), but still under 50%. Taxon DVS^{height} and DVS^{uptake} are not significantly different between the LMP, 'D' or 'E' communities ($p=0.10$

and $p=0.37$) or DVS^{height} between ‘D’ and ‘E’ communities ($p=0.03$; $\alpha=0.016$). There are no instances of large spatial-scale bivariate segregation on the ‘D’ surface and two on the ‘E’ surface (cf. [10]); Figure 2 and Supplementary Table 3). On the ‘E’ surface, spatial segregation is found between *Fractofusus* and Feather Dusters ($PCF_{Min}=0.8852$; $p=0.01$), and between Feather Dusters and *Charniodiscus* ($PCF_{Min}=0.8972$; $p=0.01$) with segregation detected between large specimens (both $p=0.01$), but not between small specimens ($p_{feaD-Fract}=0.25$ and $p_{feaD-Chard}=0.14$; Supplementary Table 3, Figure 2a,b). Therefore, habitat segregation is excluded as the underlying cause of these spatial segregations, and so they most likely reflect resource competition. For LMP, segregation occurs between Charniid I and Ostrich Feather ($PCF_{Min}=0.4932$; $p=0.01$; Figure 2d), and between Charniid II and Ostrich Feather ($PCF_{Min}=0.5346$; $p=0.01$; Figure 2c). The large specimens of Charniid II and Ostrich Feather were segregated ($p=0.01$), while small specimens were aggregated ($p=0.92$) thus resource competition is the most likely underlying process. However, the Charniid I – Ostrich Feather bivariate distribution was segregated across all size classes ($p_{small}=0.02$ and $p_{large}=0.01$; Supplementary Table 3), thus likely reflecting habitat segregation rather than competition.

If resource competition dominates community dynamics and leads to tiering, then the extent of DVS^{height} and/or $DVS^{uptake-zone}$ should predict whether two taxa exhibit inter-specific competition, with high DVS taxon pairs not competing (as they occupy different parts of the water column). This resource competition-dominated community dynamic is consistent with the ‘D’ surface community, which exhibited high DVS , and had no instances of inter-specific resource competition (Figs. 2, 3; Supplementary Table 3). However, on the ‘E’ surface, the two instances of resource competition correspond to high levels of pairwise DVS^{uptake} with respect to both Feather Dusters – *Fractofusus* and Feather Dusters – *Charniodiscus* (DVS^{uptake}_{FeaD-}

$Fract=75.1\%$; $DVS^{uptake}_{FeaD-Chard}=60.3\%$; Supplementary Table 3). On the ‘E’ surface, Charniids and *Thectardis* both exhibit very low DVS^{uptake} levels ($DVS^{uptake}_{Charniid}=10.4\%$ and $DVS^{uptake}_{Thect}=12.0\%$), but do not correspond to any of the instances of inter-specific competition identified; neither do the comparatively high levels of uptake-zone tiering correspond to the presence of resource competition (Figs. 2 and 3, Supplementary Table 1). The single LMP instance of resource competition, between Charniid II and Ostrich Feather, corresponded to a moderate level of pairwise DVS^{uptake} (38.8%), coupled to a very strong segregation ($PCF_{Min}=0.4932$). A linear regression of the DVS^{uptake} with PCF_{Min} showed no significant relationship ($p=0.283$), so our results from the ‘E’ and LMP surface provide no evidence that resource competition resulted in vertically tiered populations.

When the E’ surface taxa were subset into rangeomorphs/non-rangeomorphs, and stemmed/non-stemmed groups there were no significant differences in DVS^{uptake} or DVS^{height} between rangeomorphs and non-rangeomorphs or stemmed and non-stemmed DVS^{uptake} (Supplementary Table 2 ; all $p>>0.1$). There was a significant difference in DVS^{height} between stemmed ($DVS^{height}_{stem}=4.0\%$) and non-stemmed taxa ($DVS^{height}_{non-stem}=19.9\%$; $p=0.001$).

The development of stems has been hypothesized to enable organism uptake-zone to reach new water column heights, thus avoiding competition for resources^{7-9, 28} such as oxygen, or the dissolved organic carbon which Mistaken Point organisms likely utilised^{28,29} (see Ref [2] for further discussion). This hypothesis predicts that stemmed organisms should be more tiered (i.e. higher DVS) than non-stemmed organisms, but our results disagree: non-stemmed taxa exhibit a significantly higher degree of DVS^{height} than stemmed taxa (Supplementary Table 3). Thus, naked stems likely had a different function, such as enabling greater offspring dispersal⁷. For dispersal-generated aggregations, cluster size (Supplementary Tables 4-5) was found to strongly correlate

with maximum height of ‘E’ surface organisms ($R^2=0.997$, $p=0.034$), but not with mean height or mean uptake-zone height (all $p>>0.1$). This result demonstrates that maximum height directly resulted in greater offspring dispersal. Therefore, while stemmed organisms did not significantly benefit from the additional height for nutrient acquisition, they did gain increased offspring dispersal. While at least some Ediacaran species exhibited close-to-parent offspring dispersal due to non-waterborne, stolon dominated reproduction¹¹, evidence of wide-spread dispersal³⁰⁻³⁴ demonstrates the prevalence of Ediacaran waterborne propagation, and so the importance of colonization potential for Ediacaran macrofossils.

The lack of correlation between *DVS* and resource competition throughout Mistaken Point communities contradicts previous suggestions that competition for resources drove Ediacaran community ecology^{2-4,6, 28}. While increased height would have placed organisms in faster water flow⁸, increasing resource refresh rates, the lack of tiering within these communities demonstrates that these advantages were not significant. Additionally, we have shown that the advantage of height in these communities was a larger radius of offspring clusters – representing increased dispersal distances. Therefore, our results point to reproduction, not limited resources, as the principal driver of the dynamics of these oldest complex macro-communities.

Methods

Data. We used the data compiled by Clapham et al. (2003)^{11,35} from the Lower Mistaken Point (LMP), ‘D’ surface and ‘E’ surface which recorded the spatial position, size measurements and orientation of each fossil. Specimens were recorded as one of fourteen taxonomic groups of macrofossils, including two ‘bin’ groups³⁶: 1) *Bradgatia*, 2) *Pectinifrons*, 3) *Thectardis*, 4) *Fractofusus andersoni* + *F. misrai*, 5) *Charniodiscus spinosus* + *C. procerus*, 6) “Feather Dusters” which includes *Plumeropriscum* and *Primocandlebrum*, 7) *Hiemalora*, 8)

Ivesheadiomorphs³⁷, 9) Lobate Discs, which are interpreted either as taphomorphs (dead/decaying remains) or as microbial colonies^{2,10,17}, 10) *Charnia* ‘A’ which consists of *Beothukis mistakensis*^{38,39} (which dominates the ‘E’ surface) and *Charnia masoni*. 11) *Charnia* ‘B’ now reassigned as *Trepassia wardae*³⁹. Charniid populations on Mistaken Point are dominated by *Beothukis* (only four individuals on the ‘E’ surface are true *Charnia* species), therefore direct comparison of data from this grouping with those from other taxonomic groups should be undertaken with caution. 12) “Ostrich Feathers” 13) “Holdfast Discs”, being all discoidal specimens of uncertain affinity, with or without associated stems, which lack sufficient detail to identify the taxon, 14) “Other Species” being rare forms that do not fall into any of the other groups; e.g., *Hapsidophyllas*.

Methods. Differential erosion has the potential to distort spatial analyses⁴⁰ so this data has been tested for impact of differential erosion using heterogeneous Poisson models to model possible sources of erosion¹¹, with no significant effects found on ‘D’ and ‘E’ surfaces. In this study we fit three heterogeneous Poisson models to the LMP data, with the models dependent on x is North to South (parallel to strike), y is East to West (parallel to dip), xy is the distance from the South - East corner finding no significant erosional effect (all $p < 0.01$, where $p = 1$ corresponds to a perfect model fit – the spatial distributions depend exactly on the covariant). The tectonically distorted data was retrodeformed by returning elongated holdfast discs to a circular outline^{6,18}.

Tiering metric. We defined two different metrics for quantifying tiering: height Distinct Vertical Stratification (DVS^{height}) and uptake-zone DVS^{uptake} . DVS^{height} is calculated by 1) creating a frequency table in 1cm bins of the height of each specimen within that taxon population. 2) A similar frequency table is created using the rest of the community. 3) The two frequency tables are subtracted from each other and then 4) DVS^{height} for each taxon is calculated

as the percentage of specimens remaining divided by the total number of specimens of that taxon. Community DVS^{height} is the mean of all the taxa DVS^{height} . DVS^{uptake} is calculated similarly, but the frequency tables are created by filling in every 1cm that the specimen uptake-zone occupies. For example, a 4cm *Bradgatia* would be represented by a count in the 0cm – 4cm bin, whereas a 4cm *Charniodiscus* with a 1cm stem would be represented by a count in the 1cm – 4cm bin. For example, $DVS=0\%$ corresponds to no taxa occupying a unique part of the water column, i.e. the height distribution of that population is totally overlapped by the populations of other taxa. $DVS=100\%$ corresponds to each taxon occupying a distinct stratum of the water column, i.e. there is no overlap between specimens of any taxa.

Alternative metrics, such as overlap of a range (such as the interquartile range, or 95% standard deviations) were ruled out because such range comparisons 1) assume a distribution e.g. normal or log-normal, which isn't necessarily accurate; 2) outliers (such the giant *Fronndophyllas* found on Lower Mistaken Point) severely bias the data and 3) such range metrics do not take into account relatively frequency – many populations had relatively few specimens at the end of their height range biasing the analyses.

Specimen heights were defined as the specimen length for *Bradgatia*, Charniid I, *Thectardis*; specimen width for *Pectinifrons*; stem length plus frond length for Charniid II, Feather Dusters, *Charniodiscus* and Ostrich Feathers. *Fractofusus* height was calculated a quarter of its width, thus assuming the *Fractofusus* has two vanes. It has been suggested that *Fractofusus* had three vanes⁴¹ which would increase its vertical height. Repeating our analyses with height assuming three vanes reduces overall DVS^{height}_D by 9.3% to 70.8%, by 1.9% to $DVS^{height}_E=10.9\%$ and by 4.9% to $DVS^{uptake}_E=40.0\%$, so did not significantly change our results. Comparisons between DVS on the 'D', 'E' and LMP surfaces, and between the 'E' surface

community rangeomorphs/non-rangeomorphs and the stemmed/non-stemmed, were performed using Mann-Whitney tests. To account for the non-independence of the shared-sites in the pairwise comparisons of *DVS* on the ‘D’, ‘E’ and LMP surfaces, the significance level was set $\alpha = 0.05/3 = 0.017$, but note that such adjustment is likely to be too conservative.

Data availability. Access to the fossil localities is by scientific research permit only. Natural Areas Program, Canada for further information. Data used is publicly available at https://figshare.com/articles/Mistaken_Point_Ediacaran_count_data/1111665

Code availability. The code defining these tiering metrics has been uploaded as an R package (tiering) to <https://cran.r-project.org/>.

Spatial analyses. Initial data exploration, inhomogeneous Poisson modelling, residual analysis and segregation tests²³ were performed in R⁴² using the package spatstat⁴³⁻⁴⁵. Programita⁴⁶⁻⁵⁰ was used to find distance measures and to perform aggregation model fitting (described in detail in references^{44,46-50}).

Bivariate PCFs were calculated from the population density using a grid of 10cm x 10cm cells on the ‘D’ and ‘E’ surfaces, and 1cm x 1cm on LMP. To minimize noise a smoothing was applied to the PCF dependent on specimen abundance: A three cell smoothing over this grid was applied to the ‘D’ and ‘E’ surfaces, with five cells for LMP.

To test whether the PCF exhibited complete spatial randomness (CSR), 999 simulations were run for each relationship on a homogeneous background to generate simulation envelopes around the completely spatially random (CSR) which is where the PCF=. The fit of the fossil data to CSR was tested using Diggle’s goodness-of-fit test²² p_d (where $p_d=1$ corresponds to CSR, and $p_d=0$ corresponds to non-CSR) with PCF deviations outside the simulation envelope coupled to a $p_d < 1$ taken to indicate significantly non-CSR distributions. Note that due to non-

independence of spatial data, Monte-Carlo generated simulation envelopes cannot be interpreted as confidence intervals⁴⁷, and also run the risk of Type I errors if the observed PCF falls near the edge of the simulation envelope²¹ so that hypothesis testing needs to be further supplemented. None-the-less, if the observed data fell below the Monte-Carlo simulations, the bivariate distribution was described as segregated, and above the Monte-Carlo simulations the bivariate distribution was described as aggregated. Non-CSR distributions were tested for statistical significance using Diggle's goodness-of-fit test²², with segregations further tested using Diggle's segregation test²³ (Supplementary Table 3). Diggle's goodness-of-fit test, is a single test statistic²¹ (p_d) representing the total squared deviation between the observed pattern and the theoretical result across the studied distances. This test statistic was used in conjunction with visual inspection of Monte Carlo simulations for two reasons. First, p_d does not strictly test whether a model should be accepted or rejected, but whether the PCFs for the observed data are within the range of the stochastic realization of the model²⁶. Second, p_d depends on the range over which it is calculated. Diggle's segregation test²³, detects where two types (taxa here) are spatially segregated by calculating the sum of the square of the probability that each data point is a given type (taxa) minus the average fraction of data points which are a given type (taxa).

If a taxon was not randomly distributed on a homogeneous background, and was aggregated (Figure 2, Supplementary Table 4), the random model on a heterogeneous background was tested by creating a heterogeneous background from the density map of the taxon under consideration, being defined by a circle of radius R over which the density is averaged throughout the sample area. Density maps were formed using estimators within the range of $0.1m < R < 1m$, and the R corresponding to the best-fit model was used. If excursions outside the simulation envelopes for

both homogeneous and heterogeneous Poisson models remained, then Thomas cluster models were fitted to the data as follows:

1. The PCF and L function⁵¹ of the observed data were found. Both measures were calculated to ensure that the best-fit model is not optimized towards only one distance measure, and thus encapsulates all spatial characteristics.

2. Best-fit Thomas cluster processes⁵² were fitted to the two functions where $PCF > 1$. The best-fit lines were not fitted to fluctuations around the random line of $PCF = 1$ in order to aid good fit about the actual aggregations, and to limit fitting of the model about random fluctuations. Programita used the minimal contrast method²¹⁻²³ to find the best-fit model.

3. If the model did not describe the observed data well, the lines were refitted using just the PCF. If that fit was also poor, then only the L-function was used.

4. 99 simulations of this model were generated to create simulation envelopes, and the fit checked using the O-ring statistic⁴⁶.

5. p_d was calculated over the model range. Very small-scale segregations (under 2cm) were not included in the model fitting, since they likely represent the finite size of the specimens, and the lack of specimen overlap.

6. If there were no excursions outside the simulation envelope and the p_d -value was high, then a univariate homogeneous Thomas cluster model was interpreted as the best model.

The most objective way to resolve the number and range of size classes in a population is by fitting height-frequency distribution data to various models, followed by comparison of (logarithmically scaled) Bayesian information criterion (BIC) values⁵⁵, which we performed in R using the package MCLUST⁵⁶. The number of populations thus identified was then used to

define the most appropriate size classes. A BIC value difference of > 10 corresponds to a “decisive” rejection of the hypothesis that two models are the same, whereas values < 6 indicate only weakly reject similarity of the models⁵⁵⁻⁵⁷.

Once defined, the PCFs for each size class were calculated, and segregated tests performed. Although it was necessary to set firm boundaries for each size class, the populations are normally distributed and therefore overlap. As a result, the largest individuals of the small population are grouped within the middle size class, while some of the smallest of the medium population are included within the small size class. As such, the medium population was excluded from analyses.

For each bivariate distribution displaying segregation, the size-classes of each taxon were calculated, the bivariate PCFs of the smallest size-classes and largest size-classes were plotted with 99 Monte Carlo simulations of a complete spatially random distribution and segregation tests performed.

Regression analyses. In order to investigate the relationship between height and dispersal linear regressions were performed in R⁴¹. Programita⁴⁶⁻⁵⁰ was used to find the taxa whose univariate distributions were best modelled by Thomas Cluster models (thus most likely to be dispersal induced) and the best-fit cluster radius was used to indicate dispersal range. Four different height variables were found for each taxon’s population 1) Mean height 2) Maximum height, 3) Mean mid-point of uptake-zone and 4) Maximum mid-point of uptake zone. The uptake-zone mid-point for each specimen was calculated as the half-way point between the top of the stem and the top of the frond and was a proxy for dispersal release throughout the entire uptake-zone.

References

1. Pu, J.P., Bowring, S.A., Ramezani, J., Myrow, P., Raub, T.D., Landing, E., Mills, A., Hodgkin, E. and Macdonald, F.A.. Dodging snowballs: Geochronology of the Gaskiers glaciation and the first appearance of the Ediacaran biota. *Geology*, **44**, 955-958 (2016).
2. Liu, A. G, Kenchington C. G. & Mitchell, E. G. Remarkable insights into the paleoecology of the Avalonian Ediacaran biota. *Gondwana Res.* **27**, 1355–1380 (2015).
3. Butterfield, N. J. Animals and the invention of the Phanerozoic Earth system. *Trends in Ecology & Evolution* **26**, 81-87 (2011).
4. Woodward, G., Ebenman, B., Emmerson, M., Montoya, J.M., Olesen, J.M., Valido, A. and Warren, P.H.. Body size in ecological networks. *Trends in ecology & evolution*, **20**, 402-409 (2005).
5. Liu, A. G., McIlroy, D., & Brasier, M. D. First evidence for locomotion in the Ediacara biota from the 565 Ma Mistaken Point Formation, Newfoundland. *Geology*, **38**, 123-126 (2010).
6. Clapham, M. E., & Narbonne G. M., Gehling, J. G. Ediacaran epifaunal tiering. *Geology*, **30**, 627-630 (2002).
7. Laflamme, M., Flude, L. I., & Narbonne, G. M. Ecological tiering and the evolution of a stem: the oldest stemmed frond from the Ediacaran of Newfoundland, Canada. *Journal of Palaeontology*, **86**, 193-200 (2012).
8. Ghisalberti, M., et al.. Canopy flow analysis reveals the advantage of size in the oldest communities of multicellular eukaryotes. *Current Biology*, **24** 305-309 (2014).
9. Laflamme, M., & Narbonne, G. M.. Ediacaran fronds. *Palaeogeography, Palaeoclimatology, Palaeoecology*, **258**, 162-179 (2008).

10. Mitchell, E. G & Butterfield, N. J. Spatial analyses of Ediacaran communities at Mistaken Point. *Paleobiology*, **44**, 40-57. (2018).
11. Mitchell, E. G., Kenchington, C. G., Liu, A. G., Matthews, J. J., & Butterfield, N. J. Reconstructing the reproductive mode of an Ediacaran macro-organism. *Nature*, **524**, 343-346 (2015).
12. Clapham, M. E., Narbonne, G.M. & Gehling, J. G. Paleoecology of the oldest known animal communities: Ediacaran assemblages at Mistaken Point, Newfoundland. *Paleobiology* **29**, 527–544 (2003).
13. Landing, E., Narbonne, G.M. & Myrow, P. (eds) Trace fossils, small shelly fossils and the Precambrian–Cambrian boundary. *Bull. NY State Mus.* **463**, 1–81 (1988).
14. Narbonne, G. M. Modular construction of early Ediacaran complex life forms. *Science* **305**, 1141–1144 (2004).
15. Hoyal Cuthill, J. F. & Conway Morris, S. Fractal branching organizations of Ediacaran rangeomorph fronds reveal a lost Proterozoic body plan. *Proc. Natl Acad. Sci. USA* **111**, 13122–13126 (2014).
16. Brasier, M. D., Antcliffe, J. B. & Liu, A. G. The architecture of Ediacaran fronds. *Palaeontology* **55**, 1105–1124 (2012).
17. Liu, A. G., McIlroy, D., Antcliffe, J. B. & Brasier, M. D. Effaced preservation in the Ediacara biota and its implications for the early macrofossil record. *Palaeontology* **54**, 607–630 (2011).
18. Wood, D. A., Dalrymple, R. W., Narbonne, G. M., Gehling, J. G. & Clapham, M. E. Paleoenvironmental analysis of the late Neoproterozoic Mistaken Point and Trepassy formations, southeastern Newfoundland. *Can. J. Earth Sci.* **40**, 1375–1391 (2003).

19. Benus, A. P. Sedimentological context of a deep-water Ediacaran fauna (Mistaken Point Formation, Avalon zone, eastern Newfoundland). *Bull. NY State Mus.* **463**, 8–9 (1988).
20. Illian, J., Penttinen, A., Stoyan, H. & Stoyan, D. *Statistical Analysis and Modelling of Spatial Point Patterns* Vol. 70 (John Wiley, 2008).
21. Diggle, P. *Statistical Analysis of Spatial Point Patterns* 2nd edn (Arnold, 2003).
22. Diggle, P., Zheng, P. and Durr, P.. Nonparametric estimation of spatial segregation in a multivariate point process: bovine tuberculosis in Cornwall, UK. *Journal of the Royal Statistical Society: Series C (Applied Statistics)*, **54**, 645-658 (2005).
23. Wiegand, T., Gunatilleke, S., Gunatilleke, N. & Okuda, T. Analyzing the spatial structure of a Sri Lankan tree species with multiple scales of clustering. *Ecology* **88**, 3088–3102 (2007).
24. Levin, S. A. in *Ecological Time Series Vol.2* (eds Powell, T. M. & Steele, J. H.) 277–326 (Springer, 1995).
25. McIntire, E. J. & Fajardo, A. Beyond description: the active and effective way to infer processes from spatial patterns. *Ecology* **90**, 46–56 (2009).
26. Wiegand, T. & Moloney, K. A. *Handbook of Spatial Point-Pattern Analysis in Ecology* (CRC, 2013).
27. Murrell, D.J. and Law, R.. Heteromyopia and the spatial coexistence of similar competitors. *Ecology letters*, **6**, 48-59 (2003).
28. Hoyal Cuthill, J.F. and Conway Morris, S. Nutrient-dependent growth underpinned the Ediacaran transition to large body size. *Nature ecology & evolution*, **1**, 1201 (2017).
29. Laflamme, M., Xiao, S., & Kowalewski, M. Osmotrophy in modular Ediacara organisms. *Proc. Natl Acad. Sci. USA*, **106**, 14438-14443 (2009).

30. Darroch, S. A. F., Laflamme, M. & Clapham, M. E. Population structure of the oldest known macroscopic communities from Mistaken Point, Newfoundland. *Paleobiology* **39**, 591–608 (2013).
31. Droser, M. L. & Gehling, J. G. Synchronous aggregate growth in an abundant new Ediacaran tubular organism. *Science* **319**, 1660–1662 (2008).
32. Penny, A. M. et al. Ediacaran metazoan reefs from the Nama Group, Namibia. *Science* **344**, 1504–1506 (2014).
33. Yuan, X. et al. The Lantian biota: a new window onto the origin and early evolution of multicellular organisms. *Chin. Sci. Bull.* **58**, 701–707 (2013).
34. Hua, H., Chen, Z., Yuan, X., Zhang, L. & Xiao, S. Skeletogenesis and asexual reproduction in the earliest biomineralizing animal Cloudina. *Geology* **33**, 277–280 (2005).
35. Clapham, M. E. Ordination methods and the evaluation of Ediacaran communities. In: *Quantifying the Evolution of Early Life* (pp. 3–21). Ed. Laflamme, Marc, Schiffbauer, James D., Dornbos, Stephen Q. Springer Netherlands (2011).
36. Shen, B., Dong, L., Xiao, S. & Kowalewski, M. The Avalon explosion: evolution of Ediacara morphospace. *Science* **319**, 81–84 (2008)
37. Liu, A. G., McIlroy, D., Antcliffe, J. B. & Brasier, M. D. Effaced preservation in the Ediacara biota and its implications for the early macrofossil record. *Palaeontology* **54**, 607–630 (2011)
38. Narbonne, G. M., Laflamme, M., Greentree, C. & Trusler, P. Reconstructing a lost world: Ediacaran rangeomorphs from Spaniard's Bay, Newfoundland. *J. of Paleontology* **83**, 503–523 (2009)

39. Brasier, M. D. & Antcliffe, J. B. Evolutionary relationships within the Avalonian Ediacara biota: new insights from laser analysis. *Journal of the Geological Society* **166**, 363-384 (2009).
40. Matthews, J.J., Liu, A.G. and McIlroy, D.. Post-fossilization processes and their implications for understanding Ediacaran macrofossil assemblages. *Geological Society, London, Special Publications*, **448**, 251-269 (2017).
41. Narbonne, G.M., Laflamme, M., Trusler, P.W., Dalrymple, R.W. and Greentree, C.. Deep-water Ediacaran fossils from northwestern Canada: taphonomy, ecology, and evolution. *Journal of Paleontology*, **88**, 207-223 (2014).
42. R Core Team. *R: A Language and Environment for Statistical Computing*. R Foundation for Statistical Computing Vienna, Austria (2013)
43. Baddeley, A. & Turner, R. Spatstat: an R package for analyzing spatial point patterns. *J. of Statistical Software* **12**, 1–42 (2005)
44. Berman, M. Testing for spatial association between a point process and another stochastic process. *Applied Statistics* **35**, 54–62 (1986)
45. Baddeley, A., Rubak, E. & Møller, J. Score, pseudo-score and residual diagnostics for spatial point process models. *Statistical Science* **26**, 613–646 (2011)
46. Wiegand, T. & Moloney, K. Rings, circles, and null-models for point pattern analysis in ecology. *Oikos* **104**, 209–229 (2004)
47. Wiegand, T., Kissling, W., Cipriotti, P. & Aguiar, M. Extending point pattern analysis for objects of finite size and irregular shape. *J. of Ecology* **94**, 825–837 (2006)

48. Wiegand, T., Moloney, K., Naves, J. & Knauer, F. Finding the missing link between landscape structure and population dynamics: a spatially explicit perspective. *The American Naturalist* **154**, 605–627 (1999)
49. Loosmore, N. B. & Ford, E. D. Statistical inference using the G or K point pattern spatial statistics. *Ecology* **87**, 1925–1931 (2006)
50. Wiegand, T. & Moloney, K. A. *Handbook of Spatial Point-pattern Analysis in Ecology*. 538 pages. CRC Press (2013)
51. Levin, S. A. *The problem of pattern and scale in ecology* (pp. 277–326). Springer U.S. (1995)
52. Besag, J. Spatial interaction and the statistical analysis of lattice systems. *J. of the Royal Statistical Society. Series B (Methodological)* **36**, 192–236 (1974)
53. Thomas, M. A generalization of Poisson’s binomial limit for use in ecology. *Biometrika* **36**, 18–25 (1949)
54. Grabarnik, P., Myllymäki, M. & Stoyan, D. Correct testing of mark independence for marked point patterns. *Ecological Modelling* **222**, 3888–3894 (2011)
55. Fraley, C. & Raftery, A. E. *MCLUST version 3: an R package for normal mixture modeling and model-based clustering*. Washington University Seattle Dept of Statistics (2006)
56. Fraley, C. & Raftery, A. E. Bayesian regularization for normal mixture estimation and model-based clustering. *J. of Classification* **24**, 155–188 (2007)
57. Péliissier, R. & Goreaud, F. A practical approach to the study of spatial structure in simple cases of heterogeneous vegetation. *J. of Vegetation Science* **12**, 99–108 (2001)
58. Stoyan, D., Kendall, W. S. & Mecke, J. *Stochastic geometry and its applications*. 2nd edition. 458 pages. Springer Verlag (1995)

Acknowledgments: We thank N. Butterfield and A. Liu for discussions on this manuscript. The Parks and Natural Areas Division, Department of Environment and Conservation, Government of Newfoundland and Labrador provided permits to conduct research within the Mistaken Point Ecological Reserve in 2010, 2016 and 2017. This work has been supported by the Natural Environment Research Council [grant number NE/P002412/1], Gibbs Travelling Fellowship from Newnham College, Cambridge and a Henslow Junior Research Fellowship from Cambridge Philosophical Society to E. G. M.

Author contributions. E.G.M and C. G. K conceived the project, discussed the results and prepared the manuscript. E. G. M. conceived and ran the analyses.

The authors declare no competing interests.

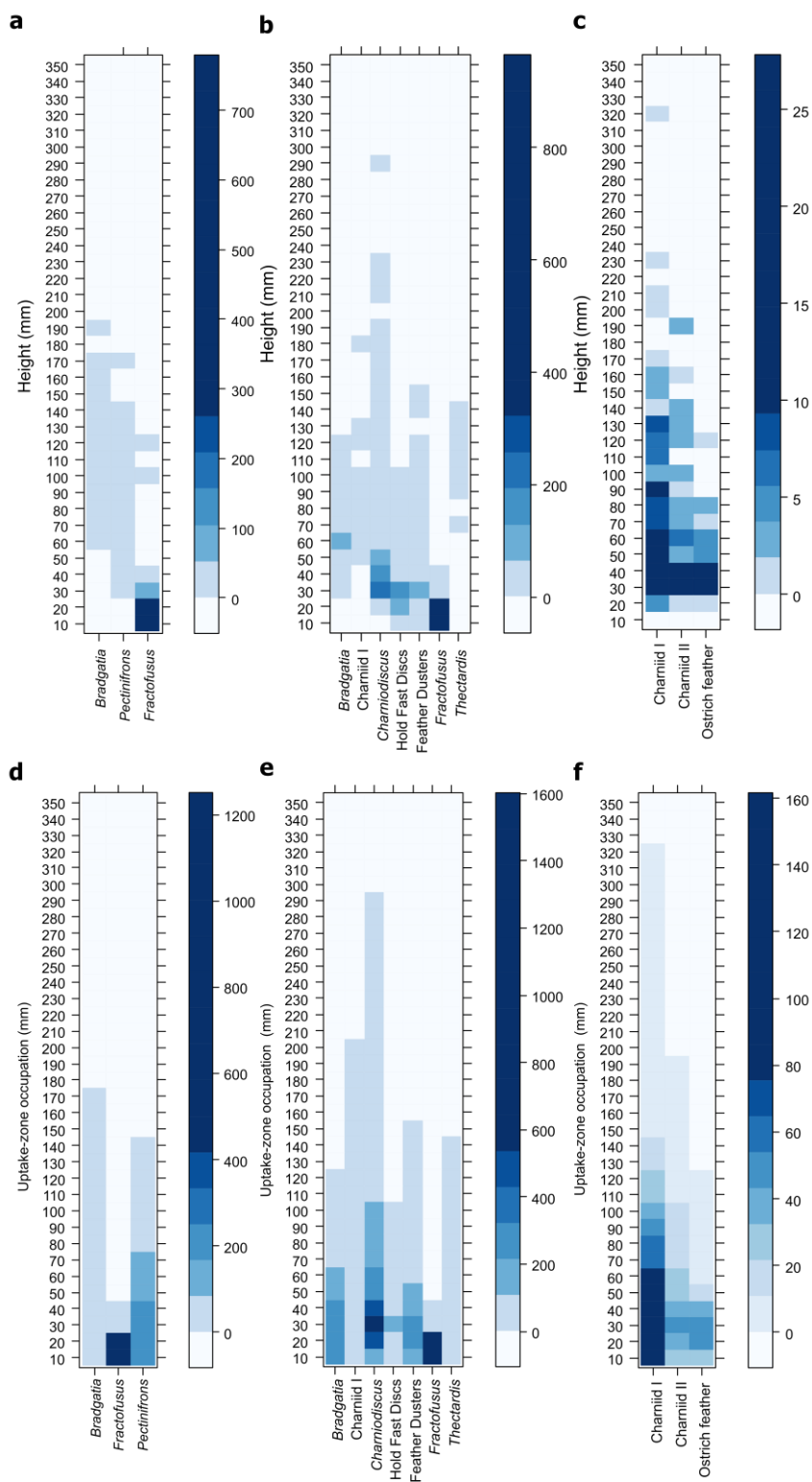


Figure 1. DVS for Mistaken Point communities. Height distributions of the **a**, ‘D’ surface community **b**, ‘E’ surface community and the **c**, LMP surface community, and uptake-zone distributions of the **d**, ‘D’ surface community **e**, ‘E’ surface community and the **f**, LMP surface community. The taxonomic group is given on the *x*-axis, and the *y*-axis is the height above the substrate in millimetres. The shade of the bin is given by the scale to the right of each community plot, and represents the frequency of specimens at the given height (**a-c**) and the occupation frequency of specimen uptake-zone (**d-f**). For example, in the height frequency plots (**a-c**), a 56mm tall specimen with or without a stem would feature in the 50-60mm box only. For the uptake-zone occupancy plots (**d-f**), a non-stemmed specimen 56mm tall would be shown in the 10, 20, 30, 40, 50 and 60mm bins. A stemmed specimen 56mm tall with a 30mm stem would be shown in the 40, 50 and 60mm bins.

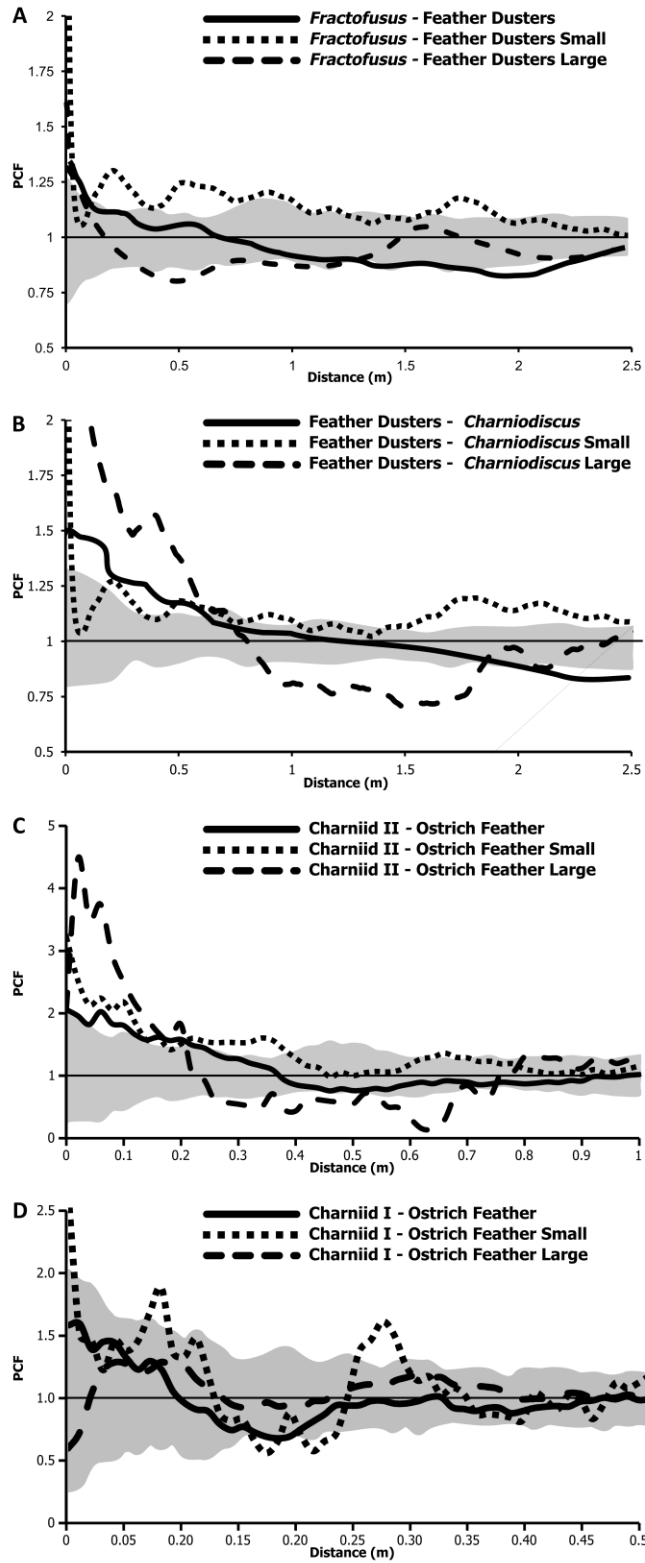
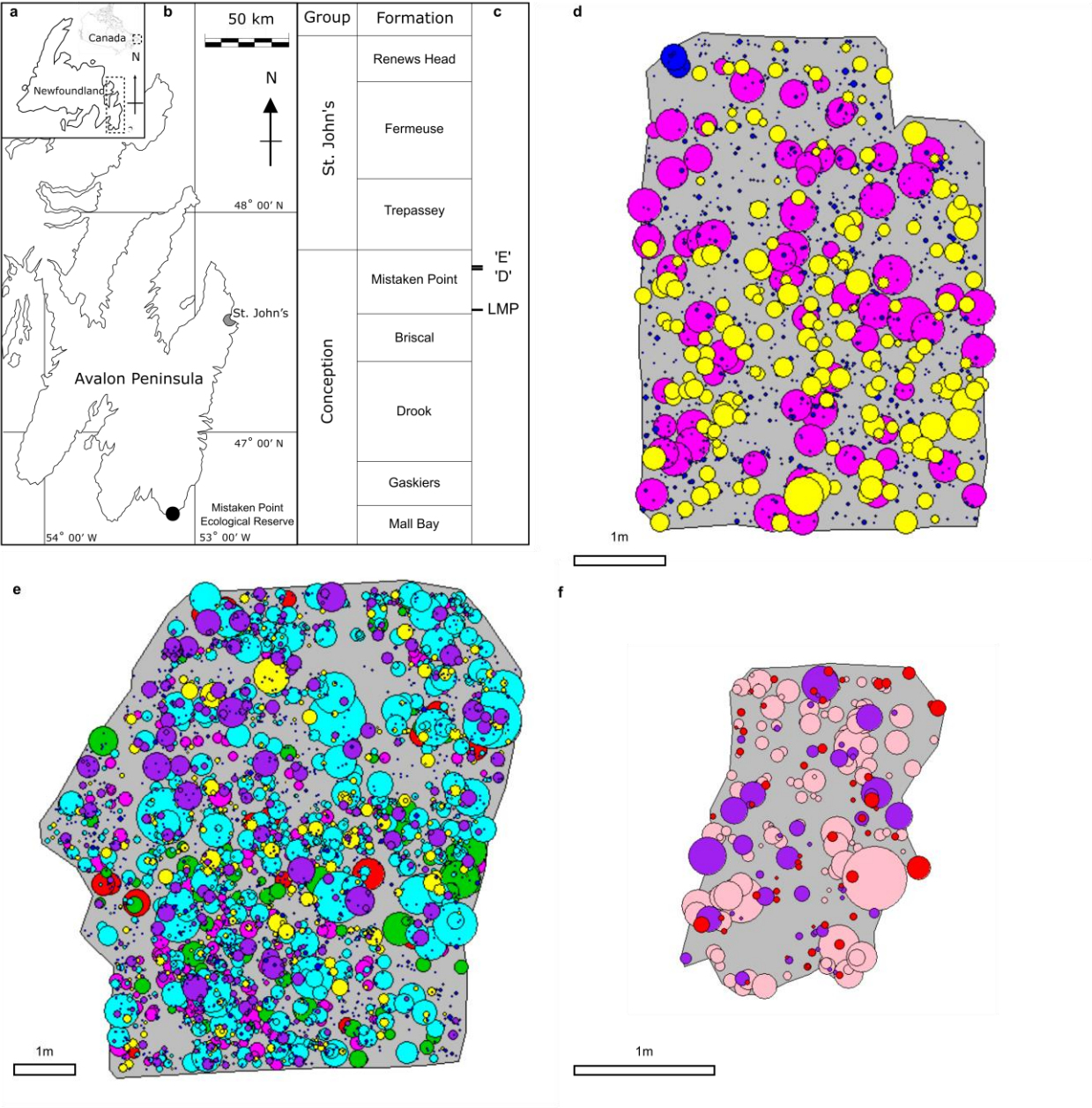
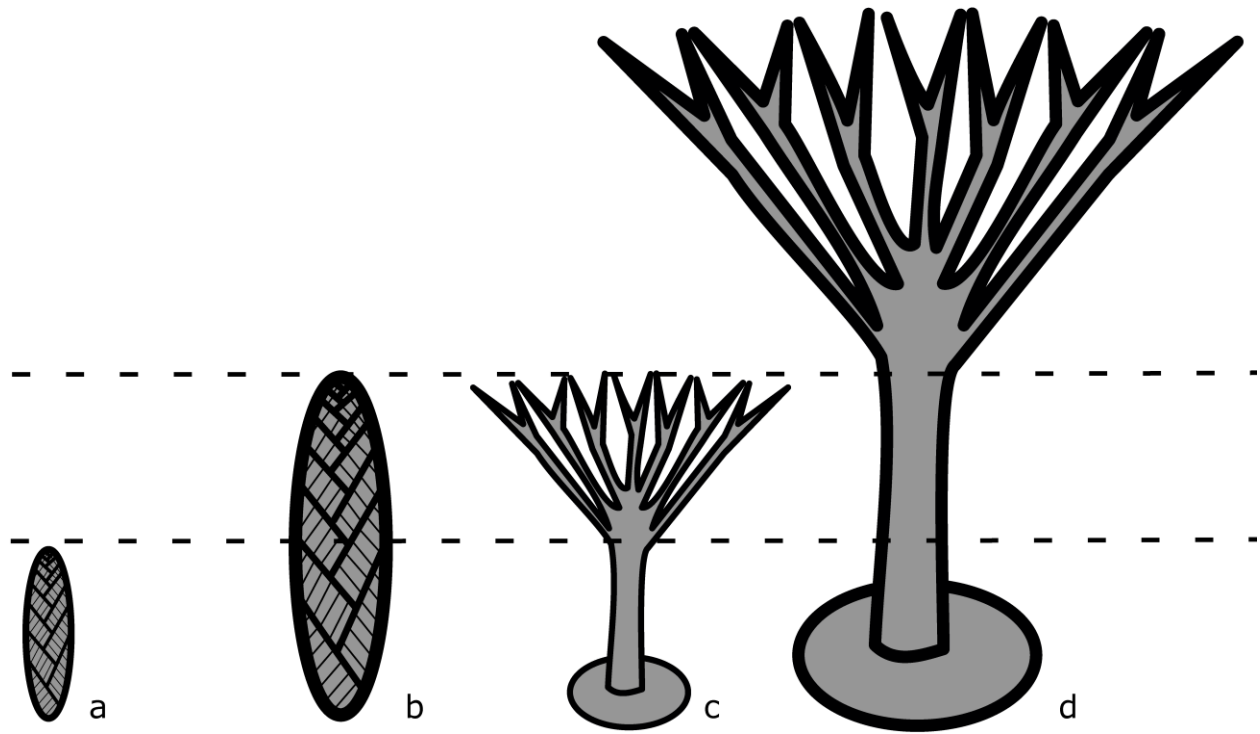


Figure 2. PCF for resource competition interactions. The x-axis is the inter-point distance between organisms in meters. On the y-axis, PCF=1 indicates CSR, <1 indicates segregation and >1 indicates aggregation. The grey shaded area denotes the boundaries of 99 Monte Carlo simulations of CSR. Since the PCF curves are not within these areas, the complete spatial randomness (CSR) hypotheses is rejected and one can assume that the distributions on both surfaces are aggregated at small spatial scales and segregated at large spatial scales. ($p_d^{Fract-FeaD} < 0.01$, $p_d^{CharI-FeaD} < 0.01$, $p_d^{CharI-IOst} < 0.01$, $p_d^{CharII-IOst} < 0.01$). **a**, PCFs for ‘E’ surface *Fractofusus* – Feather Dusters (1497 *Fractofusus* specimens of which 126 were small and 303 were large and Feather Dusters 362 specimens of which 296 were small and 66 large). **b**, PCFs for ‘E’ surface *Charniodiscus* – Feather Dusters (*Charniodiscus* 825 specimens of which 489 were small and 336 were large and Feather Dusters 362 specimens of which 296 were small and 66 large). **c**, PCF for the segregated aggregation of the LMP surface (Charniid II 51 specimens of which 26 were small and 25 were large and Ostrich Feather 54 specimens of which 38 were small and 16 large). **d**, PCF for the segregated aggregation of the LMP surface (Charniid I 143 specimens of which 47 were small and 25 were large and Ostrich Feather 54 specimens of which 38 were small and 16 large).



Supplementary Figure 1.

Map and simplified stratigraphic column showing the position of studied bedding planes with bedding plane maps. a, Newfoundland, eastern Canada. Dashed area indicates region of interest in b. **b,** The Avalon Peninsula, eastern Newfoundland. Locations of the bedding planes are indicated. **c,** Stratigraphic column (not to scale) of the Avalon Peninsulas. The ‘E’ surface at Mistaken Point has been dated to $566 \pm 0.3\text{Ma}$ (ref. 1). **d-e,** Maps of the ‘D’, ‘E’ and LMP surfaces showing specimen position and height (circle diameter). **d,** ‘D’ surface, showing *Fractofusus* (blue), *Pectinifrons* (yellow) and *Bradgatia* (Pink). **e,** ‘E’ surface with *Charniodiscus* (red), Holdfast discs with stems (orange), Charniid I (green), *Thectardis* (purple), *Fractofusus* (blue), *Bradgatia* (pink) and Feather Dusters (yellow) and **f,** Lower Mistaken Point showing Charniid A (I), Charniids II (purple) and Ostrich Feathers (red). Data from [12]. Scale bar 1m.

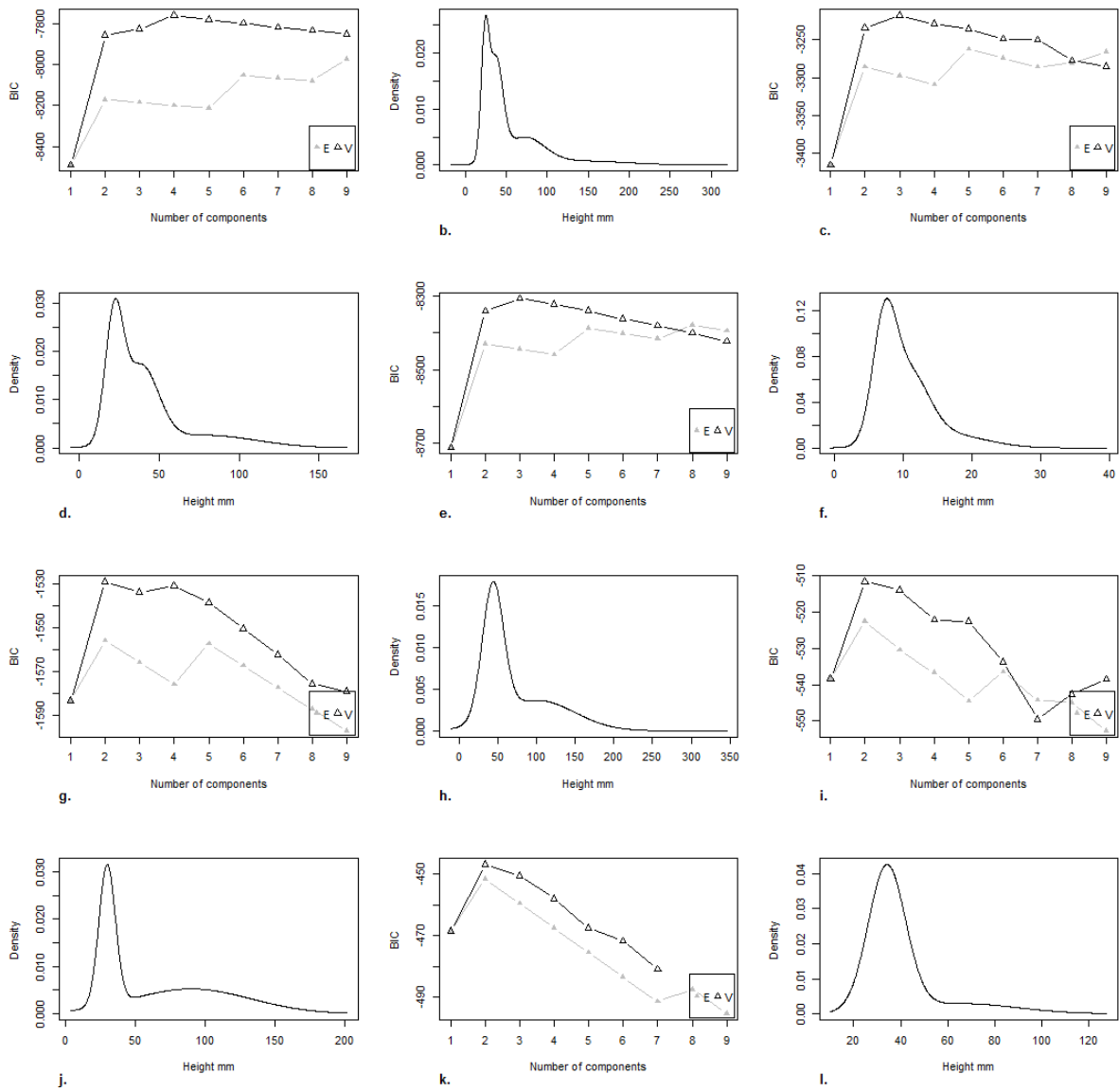


Supplementary Figure 2. Diagram illustrating DVS and uptake-zone quantification.

Uptake-zone was defined as the part of the organism which exhibited multiple scales of branching. In specimens i and ii, the uptake-zone consists of the entire height because they lack a naked stem. For specimens iii and iv, the uptake-zone is only the top 50% of the specimen, as the naked stem comprises the other 50%. To calculate *DVS*, the specimens within each taxon population were tabulated into 1cm height bins firstly using their height, and secondly their uptake-zone height ranges. For the above community (consisting of specimens i – iv), for the Charniid specimens (specimens i and ii), specimen i occupies a distinct stratum to the Feather Dusters (specimens iii and iv), while specimen ii height overlaps specimen iii in, and thus does not occupy a distinct stratum from Feather Dusters: consequently, the Charniids have a $DVS^{height} = 50\%$. For the Feather Dusters (specimens iii and iv), specimen iii overlaps with ii, so does not occupy a distinct stratum, but specimen iv is not overlapped by any Charniid specimens: so, Feather Duster $DVS^{height} = 50\%$. Community DVS^{height} is the mean of the values for all taxa in the

498 community: $DVS^{height}_{Community} = 50\%$. The uptake-zone $DVS^{uptake}_{Community} = 50\%$ as well,
499 because the uptake-zones of specimens i and iv occupy distinct strata, but ii and iii do not.

500



Supplementary Figure 3.

Size distribution analysis of taxa with segregated bivariate PCFs. Size distribution analysis of taxa with segregated bivariate PCFs. **a**, ‘E’ surface *Charniodiscus* height-frequency distributions, and **b**, the results of Bayesian Information Criterion^{54,55} (BIC). Triangles and squares correspond to models assuming equal and unequal variance respectively. High BIC values correspond to a good model fit, so the best-fit model is a three component equal variance model. **c**, ‘E’ surface Feather Dusters height-frequency distributions and **d**, BIC. **e**, ‘E’ surface *Fractofusus* height-frequency distributions and **f**, BIC. **g**, LMP Charniid I height-frequency distributions, and **h**, BIC. **i** LMP Charniid II height-frequency distributions, and (J), BIC, (K), LMP Ostrich Feathers height-frequency distributions, and **j**, BIC.

Surface Taxon	Height DVS			Uptake-zone DVS		
	D	E	LMP	D	E	LMP
<i>Bradgatia</i>	0.6184	0.0000		0.6184	0.4204	
Charniid		0.0000	0.5232		0.1071	0.6821
Charniid II			0.0784			0.2549
<i>Charniodiscus</i>		0.0776			0.5806	
Feather Dusters		0.0000			0.0359	
<i>Fractofusus</i>	0.9957	0.7963		0.9957	0.8831	
Ostrich Feather			0.0000			0.2778
<i>Pectinifrons</i>	0.8057			0.8057		
<i>Thectardis</i>		0.0000			0.1200	

Supplementary Table 1. Table of DVS values for Mistaken Point communities. Table of height and uptake-zone DVS for each taxon population within each of D, E and LMP communities. *DVS* = 0% corresponds to no specimens occupying a unique part of the water column, i.e. the height distribution of that population is totally overlapped by other taxa populations. *DVS* =100% corresponds to no overlap between any specimens, so each taxon occupies a distinct strata.

522

Surface	D	E	Lower Mistaken Point
Rangeomorph	96.96%	55.15%	71.82%
Stemmed	0.54%	30.18%	42.27%
Other	2.5%	14.67%	14.09%

523

Supplementary Table 2.

524

Community compositions. Percentage of taxa from each surface that are rangeomorphs and

525

have stemmed. The “Other category” refers to taxa which cannot be placed as either

526

Rangeomorphs or stemmed taxa due to lack of taxonomic certainty.

527

Surface	Taxon 1	Taxon 2	PCF _{min}	Size class <i>p</i> value	
				Small	Large
E	<i>Fractofusus</i>	Feather Dusters	0.8852	0.25	0.01
E	Feather Dusters	<i>Charniodiscus</i>	0.8972	0.14	0.01
LMP	Charniid I	Ostrich Feather	0.4932	0.02	0.01
LMP	Charniid II	Ostrich Feather	0.5346	0.92	0.01

Supplementary Table 3.

Segregation test for the different size-classes of segregated bivariate distributions. A value of $p < 0.05$ is significantly segregated, while $p > 0.05$ is not significantly segregated.

Surface	Taxon	σ (m)	Mean Height (mm)	Maximum Height (mm)	Mean mid-point of Uptake-zone (mm)	Maximum mid-point of Uptake-zone (mm)
E	<i>Charnidiscus</i>	0.07	54	291	30	58
E	Feather Duster	0.25	41	153	43	106
E	<i>Thectardis</i>	0.18	102	165	16	104
LMP	Charniid II	0.22	63	185	26	93
LMP	Ostrich Feather	0.18	39	118	14	34

Supplementary Table 4.

Taxon height and cluster sizes. The best-fit cluster size for the Thomas Cluster model of each frondose taxon exhibiting Thomas Cluster aggregation^{4,5}. The mid-point of the active zone height is given by calculating the mid-point between the stem and the top of the frond for each specimen.

Surface	Top of Stem Height				Uptake-zone height				Top of frond Height			
	Mean		Max		Mean		Max		Mean		Max	
	<i>p</i>	R ²	<i>p</i>	R ²	<i>p</i>	R ²	<i>p</i>	R ²	<i>p</i>	R ²	<i>p</i>	R ²
E	<i>0.47</i>	0.54	<i>0.48</i>	0.54	<i>0.78</i>	0.12	<i>0.28</i>	0.82	<i>0.88</i>	0.04	0.03	1.00

Supplementary Table 5.

Linear regression analyses. Linear regressions of the fitted cluster sizes of Table S3 for frondose organisms showing a Thomas Cluster i.e. dispersal process aggregations. The regressions which are significant are given in bold. These analyses could not be repeated for LMP surface due to insufficient sample size.